Behavioural Brain Research 417 (2022) 113618

Contents lists available at ScienceDirect

Behavioural Brain Research

journal homepage: www.elsevier.com/locate/bbr

Research report

Resting-state dynamic functional connectivity predicts the psychosocial stress response

Yadong Liu [a,b,1], Xi Ren [a,b,1], Mei Zeng [a,b], Jiwen Li [a,b], Xiaolin Zhao [a,b], Xuehan Zhang [a,b], Juan Yang [a,b,*]

[a] Faculty of Psychology, Southwest University, Chongqing 400715, China
[b] Key Laboratory of Cognition and Personality, Ministry of Education, Southwest University, Chongqing 400715, China

ARTICLE INFO

Keywords:
Resting-state
Dynamic functional connectivity
Stress response
Montreal imaging stress test

ABSTRACT

Acute stress triggers a complex cascade of psychological, physiological, and neural responses, which show large and enduring individual differences. Although previous studies have examined the relationship between the stress response and dynamic features of the brain's resting state, no study has used the brain's dynamic activity in the resting state to predict individual differences in the psychosocial stress response. In the current study, resting-state scans of forty-eight healthy participants were collected, and then their individual acute stress responses during the Montreal Imaging Stress Test (MIST) paradigm were recorded. Results defined a connectivity state (CS) characterized by positive correlations across the whole brain during resting-state that could negatively predict participants' feelings of social evaluative threat during stress tasks. Another CS characterized by negative correlations between the frontal-parietal network (FPN) and almost all other networks, except the dorsal attentional network (DAN), could predict participants' subjective stress, feelings of uncontrollability, and feelings of social evaluative threat. However, no CS could predict participants' salivary cortisol stress response. Overall, these results suggested that the brain state characterized as attentional regulation, linking self-control, and top-down regulation ability, could predict the psychosocial stress response. This study also developed an objective indicator for predicting human stress responses.

1. Introduction

Response to stress involves changes in both the subjective emotional experience [1,2] and the objective endocrine system [3]. Recently, with the development of modern technology, especially with the application of resting-state functional magnetic resonance imaging (rs-fMRI), studies have shown that functional connectivity during rs-fMRI significantly predicts the endocrine stress response [4]. Moreover, this method also helps researchers to identify adaptive stress response patterns [5] that can help predict stress-related health risks [6] and evaluate the effects of treatments on stress disorders [7,8]. Not only do these studies help researchers to better understand patterns of the stress response, but they also offer useful tools for detecting individual differences in stress.

Notably, previous studies exploring brain activity during rs-fMRI were mostly based on the 'temporal stationary' hypothesis, which considers the activation and functional connectivity in the resting state to be static during the whole scanning process [9-11]. Recent studies have found that the brain shows spontaneous activity in the resting state that fluctuate with time [12-14]. Therefore, studies have been undertaken to capture the brain's dynamic activity during resting-state [15-17]. These approaches showed high sensitivity in detecting inter-individual differences [18-22]. Researchers also argue that dynamic fluctuations of neural activity during resting-state better predict subsequent task performance [23]. Moreover, there is evidence indicating that dynamic functional connectivity is also closely related to the stress response. A previous study used the social evaluation task to induce an acute stress response, and they found that participants' emotional responses during the task were associated with the connectivity states comprising the ventromedial prefrontal cortex, amygdala, anterior insula, and anterior cingulate cortex [24]. Another study found that the brain's dynamic activity changes after acute stress [25]. However, although the brain's dynamic activity during resting-state has a high sensitivity for detecting individual differences and predicting task performance, it remains to be seen whether inter-individual differences in the characteristics of

* Corresponding author at: Faculty of Psychology, Southwest University, Chongqing 400715, China.
E-mail address: valleyqq@swu.edu.cn (J. Yang).
[1] They equally contributed to this work.

https://doi.org/10.1016/j.bbr.2021.113618
Received 6 May 2021; Received in revised form 30 September 2021; Accepted 30 September 2021
Available online 2 October 2021

dynamic activity during rest can predict stress responses.

Uncontrollability and social evaluation are two key structures that consistently induce stress responses, which include negative emotions and endocrine responses [26-28]. Notably, the frontal-parietal network (FPN) is the core structure for top-down regulation in the brain, which regulates attention, cognitive control, and emotion [29,30]. A previous study used the dynamic functional connectivity (DFC) approach to assess inter-individual differences in a stressful task and found that a connectivity state (CS) characterized by positive correlations between the FPN and brain can generate a positive emotion network [24], which may reflect participants' top-down controllability over the stress experience. In addition, positive connectivity between the FPN and default mode network (DMN) may reflect an individual's ability to regulate negative emotions, which may help people to cope with the incoming threats [30]. Moreover, positive correlations between the FPN and attentional networks, and sensorimotor networks may reflect an individual's ability to regulate attention and perception [31,32]. Thus, we hypothesized that a CS characterized by positive correlations between the FPN, DMN, attentional, and sensorimotor networks will negatively predict subsequent stress responses.

Conversely, researchers found that negative correlations between the FPN and sensorimotor networks indicate uncontrollability [33], and lower connectivity between the FPN and visual attentional network (VAN) indicates attentional deficits [34]. These findings suggest that the dysfunction of the FPN may lead to a stronger sense of uncontrollability. In addition, the DMN is the most important network during rs-fMRI, which has major functions of processing self-referential thought and mind wandering [35]. Researchers have suggested that positive correlations between the DMN and VAN represent a negative emotional state, which may involve negative thoughts about oneself [36]. During stress, an individual's perceived social-evaluative threat and uncontrollability lead to an increase in perceived stressfulness [37]. It was found that a negative emotional state before the task leads to stronger negative emotions during subsequent stress-related tasks [38]. In addition, attention deficit also leads to a higher sense of uncontrollability and lower sense of self-efficacy during subsequent tasks [39]. Therefore, we hypothesized that there will be a CS characterized by a negative correlation between the FPN and attentional network and between the sensorimotor network and VAN and that the positive correlation between the DMN and VAN will predict the subsequent stress response.

Here, we aimed to explore whether individual differences in dynamic characteristics of the brain during rest could predict the acute stress response. Firstly, participants' spontaneous brain activities during resting-state were recorded. Then, the Montreal imaging stress test (MIST) was used to induce acute psychological stress [26]. Moreover, we also set a video camera during the experiment to induce participants' feelings of social evaluative threat. After stress induction, participants were asked to retrospectively complete questionnaires that assessed their feelings of social evaluative threat and uncontrollability during the stress task. Furthermore, dynamic changes in CS were evaluated based on the results of the independent component analysis (ICA), which is considered more sensitive to individual differences [15,40,17,41,42]. If the derived CS are assumed to be mutually exclusive in time, their occurrences, and the rate of transitions between them, can be used to characterize temporal dynamics [43-45]. Based on previous studies, we hypothesized that: (1) a CS characterized by positive connectivity between the FPN and brain would negatively predict participants' stress response; (2) a CS with a negative correlation between the FPN and VAN, SMN, and VN and a positive correlation between the VAN and DMN would positively predict participants' stress response.

2. Materials and methods

2.1. Participants

Resting-state scans from 48 healthy participants were collected (mean age: 19.10 years, range 17–22, 47.8% female). Exclusion criteria consisted of psychological disorders, severe physical illness, head injury, and a history of alcoholism or drug abuse. Female participants were tested during their luteal phase (around ten days before menstruation) and did not use oral contraceptives leading up to the experiment [46,47]. All participants were asked not to eat, exercise, drink wine or coffee, or brush their teeth for one hour before the experiment was conducted. Participants have compensated 50 yuan for attending the experiment. All participants provided written informed consent and received monetary compensation. This study was approved by the review board of the local university.

2.2. Data acquisition

2.2.1. Subjective reports

Participants self-reported subjective stress levels on a 7-point Likert scale ranging from 1, corresponding to 'Not stressful', to 7, corresponding to 'Terribly stressful'. To test whether the experiment successfully induced a subjective stress response, self-reported subjective stress report was assessed repeatedly for seven times along with salivary cortisol collection. Measurement of uncontrollability and social evaluative threat (SET) were collected immediately after stress induction, wherein participants were asked to evaluate the degree of uncontrollability and the social evaluative threat they had felt during the stress induction. Uncontrollability and SET were measured on 7-point Likert scales, from 1, corresponding to 'not at all', to 7, corresponding to 'totally'.

To exclude the possible effect of either anxiety or depression, we also measured anxiety and depression in the participants. Anxiety was measured using the 40-item State-Trait Anxiety Inventory (STAI), half of which were used to estimate participants' trait anxiety. Participants were asked to rate the anxiety they felt in general on a 4-point Likert scale [48], from 1, corresponding to 'not at all', to 4 'very much so'. Participants' depression was measured by the Beck Depression Inventory (BDI), which consists of 21 items presented in a multiple-choice format that measures the presence and degree of depression in adolescents and adults [49]. Each item is evaluated using scores 0–3. Severity of depression increases with the score.

2.2.2. Salivary cortisol data acquisition

Saliva samples were collected with a sampling device (Salivette, SARSTEDT, Germany) to assess cortisol levels throughout the experiment. All saliva samples were stored at room temperature until completion of the experiment, after which they were stored at −20 °C until analysis. Cortisol concentrations were analyzed using an ELISA kit (IBL-Hamburg, Germany) following the manufacturer's instructions. The sensitivity of the cortisol assay was 0.005 μg/dl, and the inter- and intra-assay coefficients of variation for the cortisol assay were 3.2% and 6.1%, respectively.

2.2.3. fMRI data acquisition

Functional and anatomical whole-brain images were acquired using a 3 T Siemens Trio MRI scanner. We acquired 242 vol-functional images from each subject with a T2*-weighted gradient echo-planar imaging sequence during resting-state. We obtained 32 echo-planar images per volume sensitive to blood oxygenation level-dependent contrast (repetition time: TR = 2000 msec, echo time: TE = 30 msec, 64 × 64 matrix with 3 × 3 × 3 mm^3 spatial resolution, FOV = 192 × 192mm2). Slices were acquired in an interleaved order and oriented parallel to the AC-PC plane with a 0.99 mm gap. High-resolution T1-weighted 3D fast-field echo sequences were obtained for anatomical reference (176 slices, repetition time: TR = 1900 msec; echo time: TE TE = 2.52 msec; slice thickness = 1 mm; FOV = 256 mm × 256 mm; voxel size = 1 mm × 1 mm × 1 mm).

2.3. Experiment procedure

To mediate the effect of cortisol rhythm on experimental results, participants were required to arrive at the laboratory in the mid-afternoon between 3:00 and 5:00 pm. After arriving at the laboratory, participants were asked to rest for 30 min before entering the MRI scanner. A TI image was acquired first, followed by a resting-state image. Immediately afterward, the Montreal Imaging Stress Test (MIST) paradigm was used to induce a stress response for 30 min. The MIST is a well-validated tool to induce psychosocial stress during fMRI scanning. In this experiment, participants were asked to answer arithmetic questions with a time limit and visible progress bar, leading to a higher rate of incorrect responses. Participants could also see an expert on the screen who was monitoring their performance, which induced social evaluative threat. After the stress induction was completed, participants stayed in the scanner and were asked to evaluate the degree of uncontrollability and social evaluation threat they experienced during stress induction. Then participants were allowed another 25 min to rest before leaving the laboratory (Fig. 1). Both the subjective stress and salivary cortisol reports were collected inside the scanner with the help of another experimenter.

2.4. fMRI data processing

2.4.1. Data preprocessing

fMRI data was processed with MATLAB software using the Gretna toolbox [50]. The first 5 frames were removed to allow for signal stabilization. Images were then slice–time corrected, realigned, spatially normalized to the Montreal Neurological Institute template using dartel segments, and smoothed using a 4 mm full-width at half-maximum Gaussian kernel.

2.4.2. Group independent component analysis and component identification

A data-driven group spatial independent component analysis (ICA) was performed using Group ICA in the fMRI Toolbox (GIFT) ([51]; http://mialab.mrn.org/software/gift/) in the preprocessed rs-fMRI data. First, the total independent component (IC) numbers were estimated to be 34 by GIFT using the MDL criterion [52]. Then, principal components (PCs) were obtained for subject-specific data by principal component analysis (PCA). In the group-level data reduction, group data formed by the concatenation of participants' reduced data were further decomposed into fewer PCs using PCA. The Infomax ICA algorithm [53] was then used to obtain ICs. The reliability of the decomposition was evaluated by repeating the algorithm 20 times using ICASSO [53]. For each independent component, subject-specific spatial maps and time-courses were acquired using the GICA back-reconstruction algorithm [54]. Finally, 34 group-level independent components were acquired. All ICs were reconfirmed to make sure that selected ICs could reflect neuronal activity based on several principles: first, we selected ICs whose peak coordinates in the spatial maps were located in the gray matter; second, we removed ICs that highly overlapped with known vascular, ventricular, motion, and susceptibility artifacts; and finally, we selected ICs which were dominated by low-frequency fluctuations [55]. To better group ICs into different brain networks, multiple regression analyses between all ICs and prior templates [56] were conducted. Eventually, 10 ICs were selected and further categorized into eight different brain networks: the default mode network (DMN), ventral attention network (VAN), dorsal attention network (DAN), left the frontal network (LPN), right frontal network (RFN), sensorimotor network (SMN), visual network (VN), and auditory network (AN) (Fig. 2). The regression results between the 10 ICs and brain networks are listed in Table 1.

2.4.3. Siding window analysis and k-means clustering

A sliding window approach was used to calculate the DFC with the Temporal dynFN toolbox in GIFTv3.0b software (version 3.0b, https://trendscenter.org/software/gift/). Before calculating correlations between each component time series, post-processing steps were taken to remove remaining noise sources from each time series [57]. These steps included nuisance regression of the six realignment parameters and their temporal derivatives, linear, quadratic, and cubic detrending, and the removal of low-frequency trends (high-frequency cutoff of 0.15 Hz). In addition, outlier movement "spikes" were removed.

We applied a sliding window of 30 TRs (the 60S) with a Gaussian alpha value ($\sigma = 3$TRs) and a step between windows of 1TR along with the 237-TR length scan, yielding a total of 207 overlapping windows for each participant [58]. For each window, the 10×10 pair-wise covariance matrix was calculated using the graphical LASSO framework. To assess patterns of functional connectivity that reoccur over time across different participants, k-means clustering was applied to the windowed covariance matrices from all windows. The optimal number of clusters k was chosen based on the elbow criterion of the cluster validity index, computed as the ratio of intra-cluster to inter-cluster distance [57]. The clustering algorithm was repeated 500 times in Matlab with random initializations of cluster centroid positions to obtain a stable solution. In addition to using the optimal value for k, the analyses were repeated for k ranging from 2 to 8 to assess the robustness of the results regarding different values of k. We then derived three indicators to describe dynamic changes, including (1) number of transitions, which represents the overall number of transitions between different states; (2) mean dwell time, which was calculated using the average number of consecutive windows assigned to a state; and (3) the fraction of time, which was calculated using the proportion of windows assigned to a state.

2.5. Linear regression

All statistical analyses were performed using SPSS (version 22). Linear regression was performed to explore the effects of dynamic brain activity during resting-state on stress responses, after controlling for age, anxiety, and depression. All regressions were conducted separately. The brain activity could be characterized by three indicators derived from resting-state MRI data (number of transitions, mean dwell time, and fraction of time). Stress response was characterized by both subjective

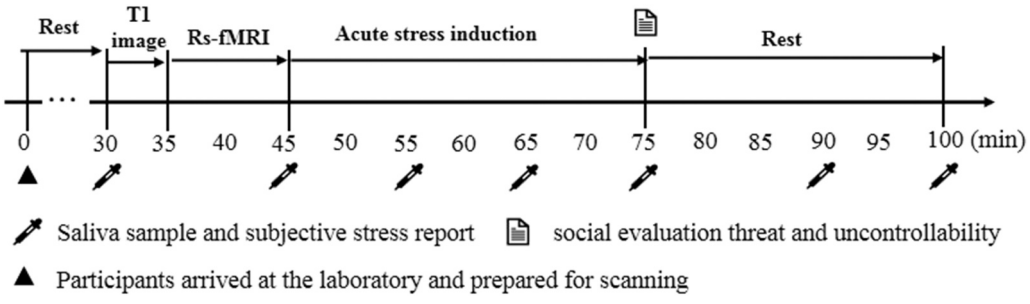

Fig. 1. An overview of the experiment procedure.

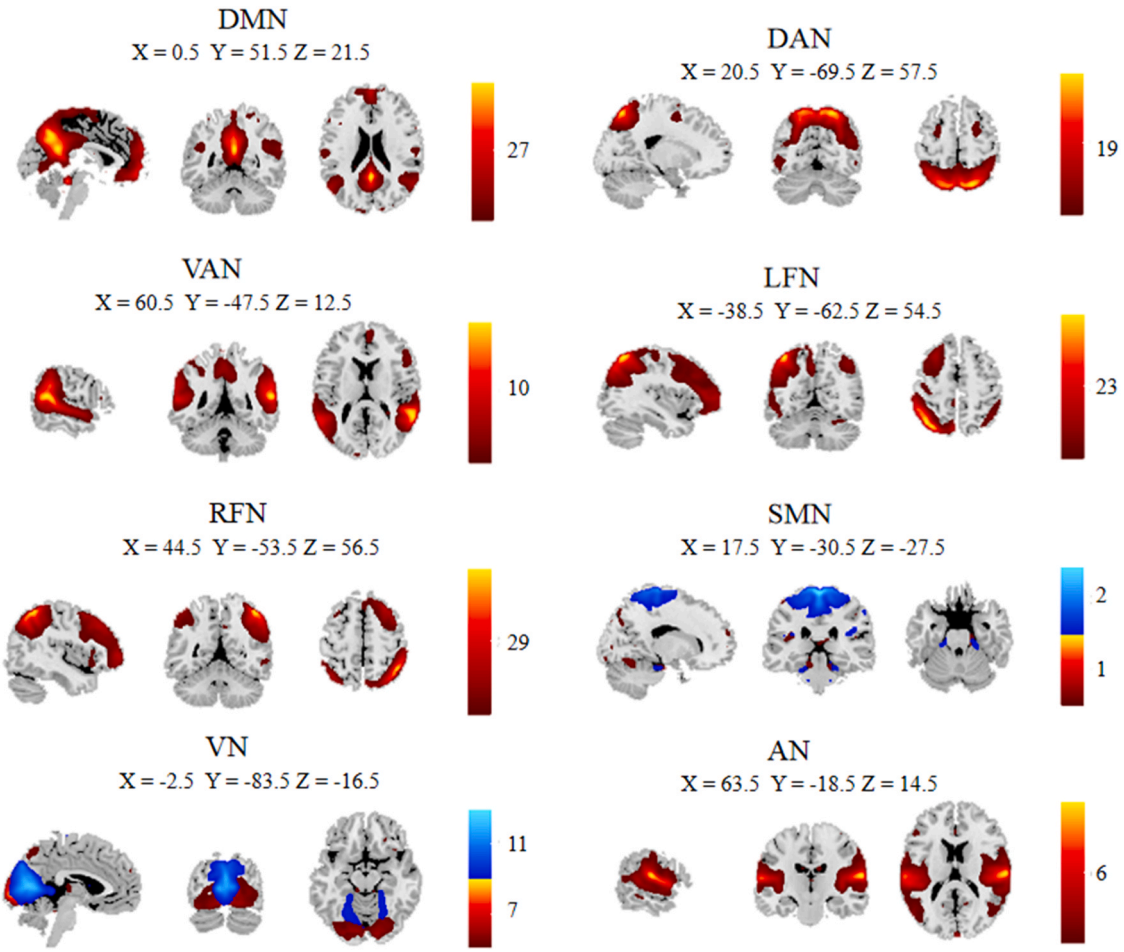

Fig. 2. Ten independent components (ICs) were selected and categorized into 8 different brain networks. Which are: default mode network (DMN), ventral attention network (VAN), dorsal attention network (DAN), left the frontal network (LPN), right frontal network (RFN), sensorimotor network (SMN), visual network (VN), and auditory network (AN); different colors represent different ICs in one network; specific IC numbers are listed next to the color bar.

Table 1
Regression analyses between prior templates and independent component (ICs).

	DMN	DAN	VAN	LFN	RFN	SMN		VN		AN
IC number	27	19	10	23	29	1	2	11	7	6
Regression results	0.45	0.41	0.28	0.28	0.46	0.3	0.31	0.55	0.35	0.57

DMN = default mode network; DAN = dorsal attention network; VAN = ventral attention network; LFN = left the frontal network; RFN = right frontal network; SMN = sensorimotor network; VN = visual network (VN); AN = auditory network.

(subjective stress reports, uncontrollability, and social evaluative threat) and endocrine (salivary cortisol) parameters. In particular, as we collected subjective stress reports and salivary cortisol repeatedly, areas under the curve with respect to increase (AUCi) were used to estimate pronounced changes in response to acute stress (both subjective and endocrine). Specifically, the first time points of these data were considered as baseline, and the AUCi compared with baseline was calculated to reflect the overall level of the stress response [59,60].

2.6. Validation analysis

Previous studies have argued that results derived from the DFC approach are susceptible to parameter settings, such as sliding window length (WL) and cluster numbers. To date, there is no consensus on the optimal length of sliding window size. Some researchers suggest that the window size setting should be between 30 and 60 s [61]. A window length of 44 s is a commonly used setting in similar studies. Therefore, in addition to the window size of 60 s in the main study, we also used a window size of 44 s to validate our results. Besides window length, we also changed the cluster numbers from k = 5 to k = 4 to exclude the influence of parameter settings on the experimental results.

3. Results

3.1. Demographic and behavioral data

Participants' subjective stress reports and salivary cortisol responses are illustrated in Fig. 3. Due to outliers in the cortisol data (more than 3 standard deviations outside the mean, both female), data from 46 participants (mean age: 19.11 years, range: 17–22, 47.8% female) were included in salivary cortisol statistical analysis [62]. Time period was determined to be a significant intra-subject variable in subjective stress self-reports, F (6282) = 81.78, $p < 0.001$, $\eta_p^2 = 0.635$. A post-hoc analysis revealed that participants reported the highest levels of perceived stress after the stress induction ($p_{time3\text{-}time1} < 0.001$, $p_{time4\text{-}time1} < 0.001$, $p_{time5\text{-}time1} < 0.001$, $p_{time5\text{-}time2} < 0.001$, $p_{time5\text{-}time3} < 0.001$,

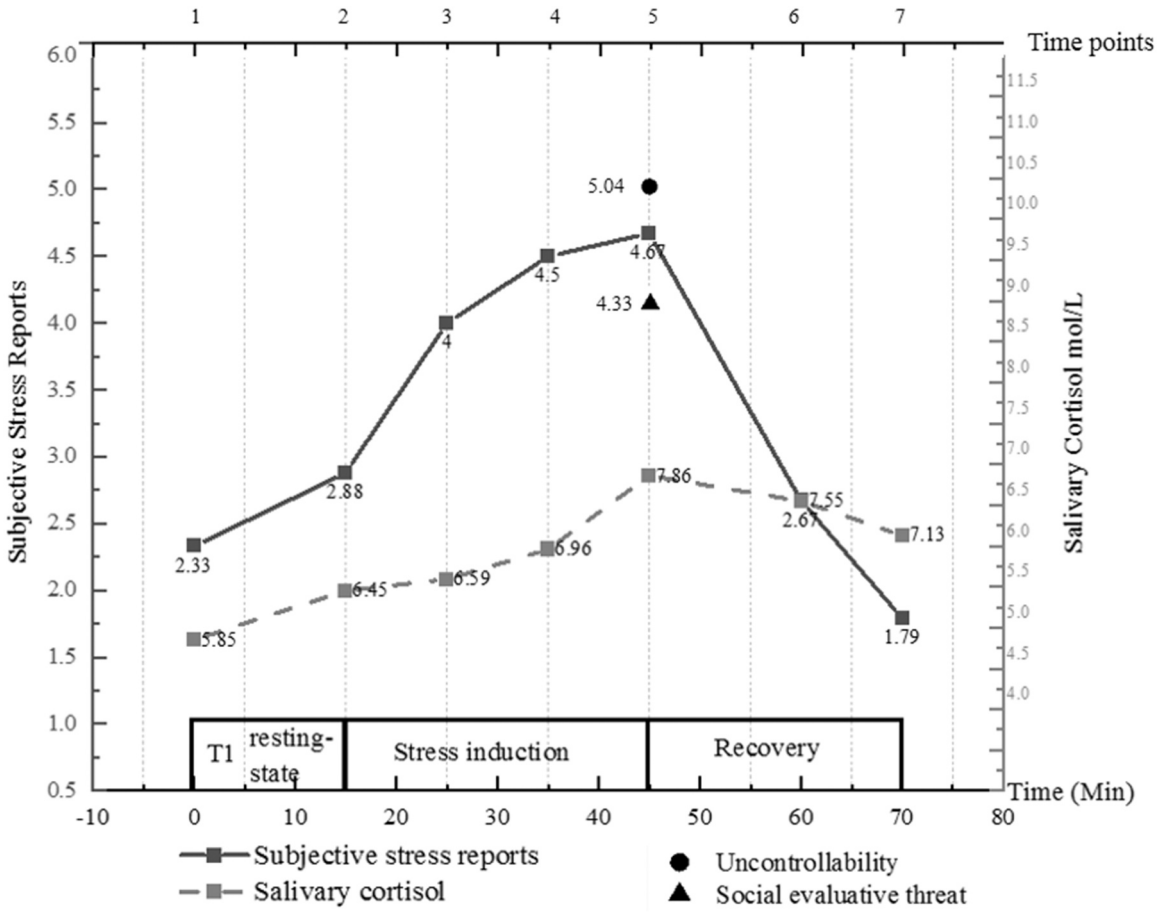

Fig. 3. Subjective stress and salivary cortisol at seven-time points.

$p_{time5\text{-}time6} < 0.001$, $p_{time5\text{-}time7} < 0.001$). Time period was also found to be a significant variable in salivary cortisol levels, F (6270) = 2.615, $p = 0.018$, $\eta_p^2 = 0.55$. A post-hoc analysis revealed that participants' salivary cortisol levels peaked after stress induction ($p_{time5\text{-}time1} < 0.05$, $p_{time5\text{-}time2} < 0.05$, $p_{time5\text{-}time3} < 0.05$, $p_{time5\text{-}time4} < 0.05$, $p_{time6\text{-}time1} < 0.05$). The reported increase of subjective stress and salivary cortisol indicate that participants' stress response was successfully induced. To describe participants' overall stress response, the area under the curve with respect to these increases was computed and listed in Table 2.

3.2. K-means clustering results

The optimal number of clusters k was estimated to be 4 using the elbow criterion (Fig. 4), indicating that there were four distinct states during the resting-state scan. State 1 accounted for 22% fraction of the resting-state scans, which meant that 22% of the windows were considered to belong to state 1. State 1 was characterized by positive correlations across the whole brain. Specifically, the frontal networks (both the left and right) were positively correlated with the DMN (IC 27), DAN (IC 19), and VAN (IC 10). Furthermore, in state 1, the DAN, VAN, LFN (IC 23), and RFN (IC 29) were positively correlated with SMN (IC 1 and 2), VN (IC 7 and 11) and AN (IC 6); moreover, the SMN, VN, and AN were positively correlated with each other. State 2 (21%) was characterized by negative correlations between the frontal networks (both the left and right) and the SMN, VN, and AN; the frontal networks were also negatively correlated with the VAN but positively correlated with DAN, whereas the DMN exhibited an inverse relationship with DAN and VAN. Finally, VAN was positively correlated with the SMN, VN, and AN. State 3 (13%) showed similar connectivity patterns to state 1; for example, they both displayed positive correlations across the whole brain. However, there were clear distinctions between states 1 and 3. Firstly, the positive correlation in state 3 was much stronger than in state 1; the DMN in state 3 was positively correlated with all other networks except the RFN, and the RFN was negatively correlated with all other networks. State 4 (44%) was characterized by positive correlations between the DMN, DAN, VAN, LFN, and RFN and between the SMN, VN, and AN.

3.3. Linear regression analyses of dynamic brain activity and stress responses

The results of the linear regression analysis of dynamic brain activity

Table 2
Descriptive data of the stress response.

	Age_{48}	SET_{48}	$Uncon_{48}$	$Depression_{48}$	$Ttait\text{-}anxiety_{48}$	$SSAUCi_{48}$	$CortiAUCi_{46}$
Mean	19.1	4.33	5.04	7.69	44.25	75.73	2.86
SD	1.1	1.43	1.03	5.67	5.27	63.03	9.57

$SSAUC_i$, $CortiAUC_i$ represent the areas under the curve with respect to increase of the seven time-points of subjective stress reports and salivary cortisol, respectively; Uncon = uncontrollability; SET = social evaluation threat; SD = standard deviation. Numbers represent the number of participants included in the analyses.

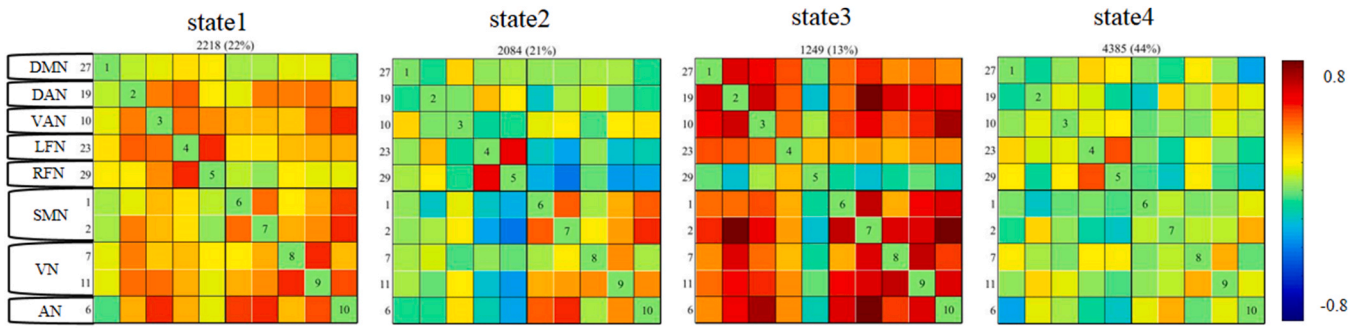

Fig. 4. Four different states reoccurred during the resting-state scan.

on the stress response are shown in Table 3 (uncorrected). One participant's (male) data were excluded (because its dynamic feathers were more than 3 standard deviations outside the mean). For state 1, results showed that the mean dwell time of state 1 had a significant effect on participants' social evaluative threat during acute stress, $\beta = -0.48$, $SE = 0.01$, $p < 0.001$, and the fraction of time of state 1 had the same effect on the social evaluative threat measurement, $\beta = -0.41$, $SE = 0.91$, $p = 0.003$. These data indicate that both longer dwell time and a greater fraction of time spent in state 1 could negatively predict participants' social evaluative threat levels during acute stress. For state 2, the mean dwell time of state 2 had a significant effect on the subjective stress increase during stress, $\beta = 0.32$, $SE = 0.52$, $p < 0.05$, indicating that longer the dwell time of state 2, the stronger the participants' subjective stress. These results also showed that the fraction time of state 2 had a significant effect on both participants' social evaluative threat, $\beta = 0.33$, $SE = 1.02$, $p < 0.05$, and feelings of uncontrollability during acute stress, $\beta = 0.34$, $SE = 0.68$, $p < 0.001$, which indicate that greater the fraction of time spent in state 2, more the social evaluative threat and uncontrollability participants felt during acute stress (Fig. 5). For state 3 and state 4, their dynamic features didn't show significant effects on the stress response.

3.4. Validation analysis

To exclude the influence of parameter settings on experimental results, we used parameters to test our main results. Similar CSs were produced when applying a sliding window length of 44 s or k = 5 (Fig. 6). Correlation results also showed a similar relationship between brain activity during resting-state and individual stress response, except for uncontrollability when k = 5. However, the change in sliding

Table 3
Linear regression analyses of dynamic brain activity and stress responses.

Predictors	SSAUCi			SET			Uncon		
	B	*SE*	*t*	*B*	*SE*	*t*	*B*	*SE*	*t*
Age	1.51	8.81	0.17	0.04	0.16	0.22	-0.15	0.13	-1.2
Trait-anxiety	0.65	1.87	0.35	0.04	0.03	1.26	0.04	0.03	1.54
Depression	0.47	1.73	0.27	0.07	0.03	2.28*	0.06	0.03	2.4*
State1_dwell	-0.91	0.66	-1.37	-0.05	0.01	-3.93**	-0.01	0.01	-0.87
Age	4.06	8.44	0.48	0.14	0.18	0.78	-0.13	0.12	-1.03
Trait-anxiety	0.9	1.81	0.5	0.04	0.04	1.13	0.04	0.03	1.69
Depression	1.26	1.7	0.74	0.09	0.04	2.48*	0.07	0.02	2.77*
State2_dwell	1.18	0.52	2.25*	0.02	0.01	1.97	0.01	0.01	1.74
Age	1.72	8.69	0.2	0.1	0.19	0.53	-0.15	0.13	-1.21
Trait-anxiety	0.91	1.86	0.49	0.04	0.04	1.09	0.04	0.03	1.64
Depression	0.55	1.72	0.32	0.08	0.04	2.11*	0.06	0.02	2.45*
State3_dwell	0.72	0.44	1.64	0.01	0.01	1.37	0.01	0.01	1.14
Age	3.67	9.35	0.39	0.09	0.2	0.48	-0.13	0.13	-1
Trait-anxiety	0.54	1.91	0.28	0.03	0.04	0.86	0.04	0.03	1.48
Depression	0.57	1.78	0.32	0.08	0.04	2.01*	0.06	0.03	2.4*
State4_dwell	-0.04	0.23	-0.17	0	0	0.52	0	0	-0.08
Age	2.65	8.96	0.3	0.06	0.17	0.36	-0.16	0.12	-1.3
Trait-anxiety	0.55	1.9	0.29	0.04	0.04	1.1	0.04	0.03	1.58
Depression	0.43	1.78	0.24	0.06	0.03	1.88	0.06	0.02	2.26*
State1_frac	-23.69	47.79	-0.5	-2.89	0.91	-3.16**	-1.09	0.66	-1.65
Age	4.72	8.57	0.55	0.16	0.18	0.92	-0.11	0.12	-0.92
Trait-anxiety	0.7	1.82	0.38	0.04	0.04	1.08	0.04	0.03	1.72
Depression	1.25	1.73	0.72	0.1	0.04	2.65*	0.07	0.02	3.06**
State2_frac	96.21	49.13	1.96	2.46	1.02	2.41*	1.74	0.68	2.56**
Age	2.68	8.88	0.3	0.11	0.18	0.57	-0.14	0.13	-1.11
Trait-anxiety	0.84	1.93	0.43	0.05	0.04	1.21	0.04	0.03	1.55
Depression	0.41	1.76	0.23	0.07	0.04	1.96	0.06	0.03	2.36*
State3_frac	45.9	57.74	0.8	1.76	1.2	1.46	0.36	0.83	0.44
Age	4.46	8.77	0.51	0.13	0.19	0.69	-0.13	0.13	-1
Trait-anxiety	0.87	1.88	0.46	0.04	0.04	0.94	0.04	0.03	1.57
Depression	0.97	1.76	0.55	0.08	0.04	2.09*	0.06	0.03	2.51*
State4_frac	-46.62	33.47	-1.39	-0.23	0.73	-0.32	-0.34	0.49	-0.7

SSAUCi = the area under the curve with respect to increase (AUCi) of the seven time-points of subjective stress reports; Uncon = uncontrollability; SET = social evaluation threat, SE = standard error, CI = confident interval;

* $p < 0.05$;

** $p < 0.01$.

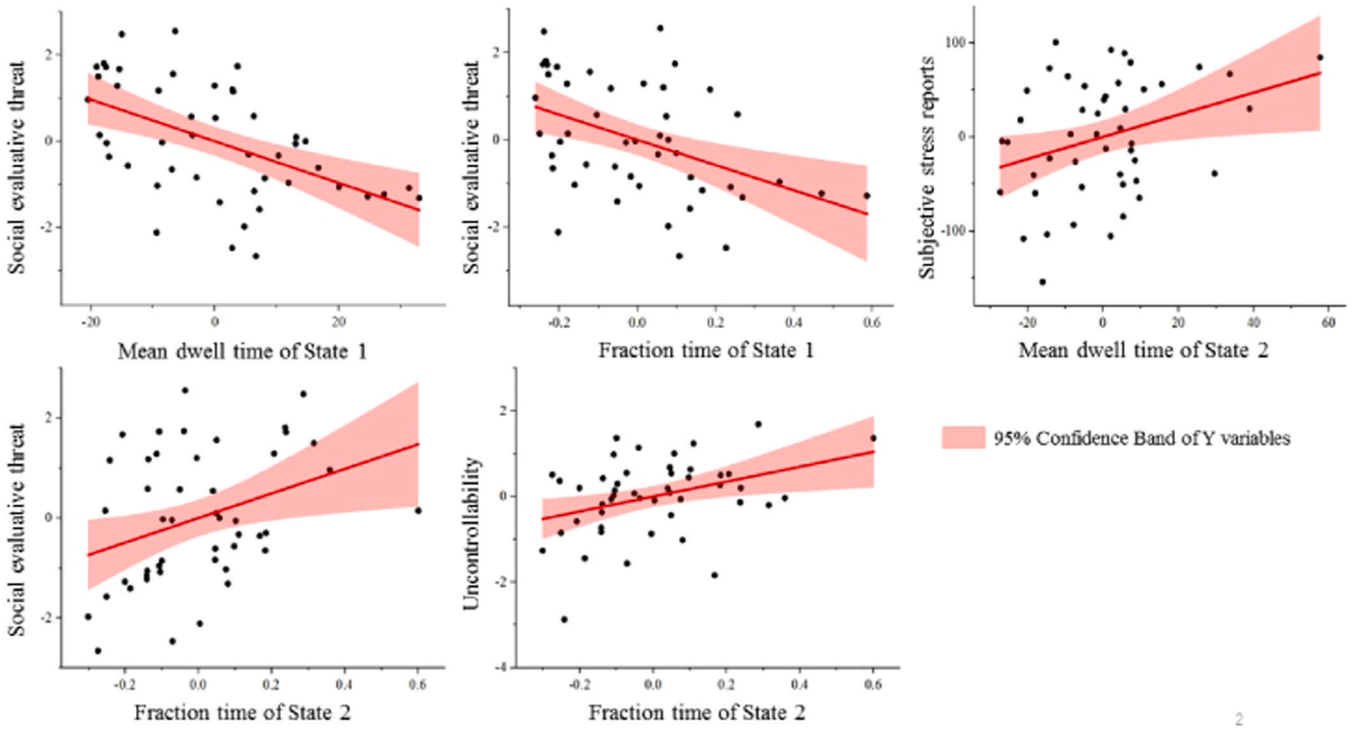

Fig. 5. Correlations between brains' dynamic activities and stress responses.

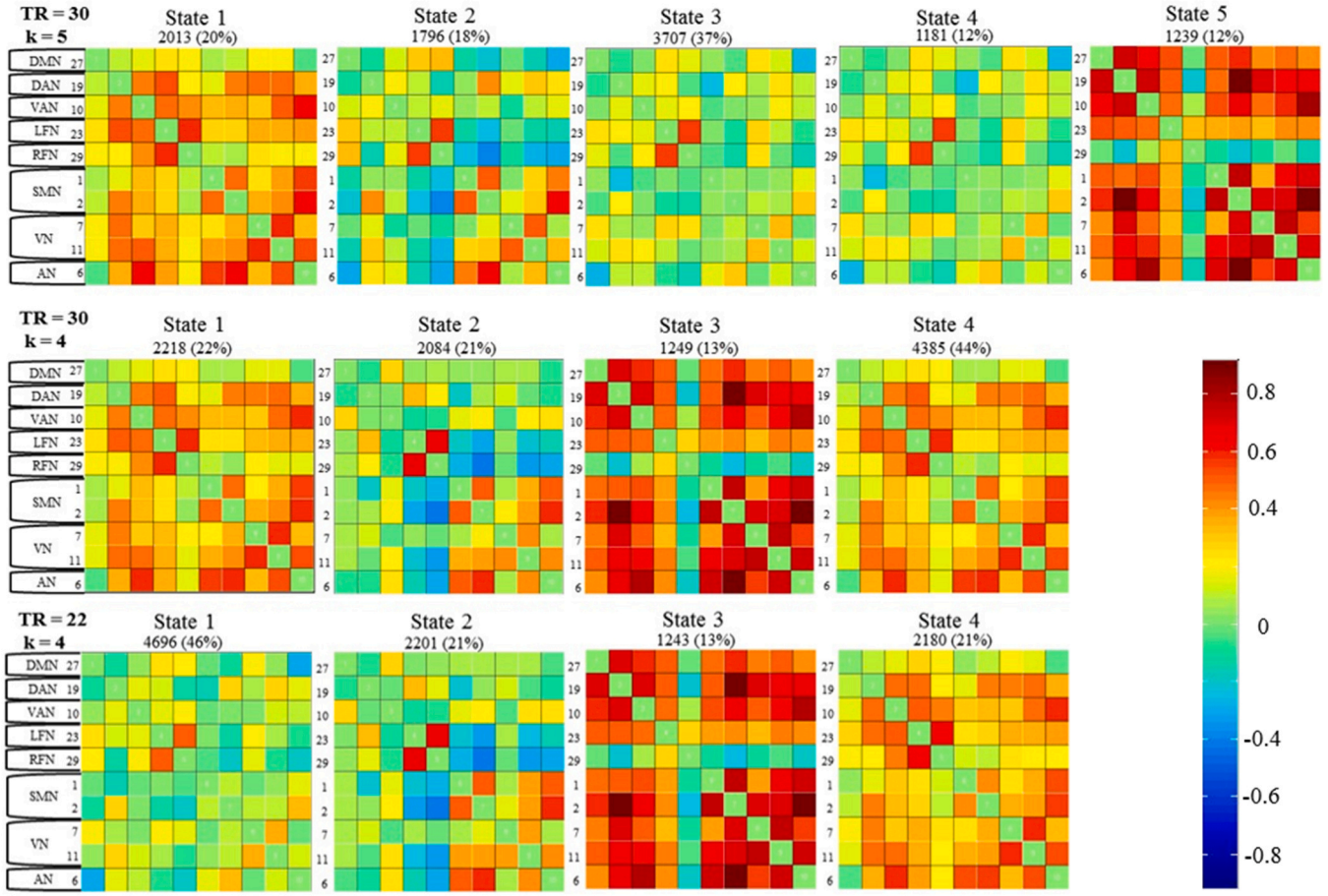

Fig. 6. Dynamic functional connectivity states derived from different parameters.

window length did not affect the main results (Table 4). Overall, changing the DFC parameter did not impact the main results.

4. Discussion

In the current study, we investigated the relationship between spontaneous brain activity during resting-state and the stress response. Our results showed that the dynamic changes during resting-state significantly predicted individual participants' subjective stress response. Specifically, the mean dwell time of a state characterized by positive correlations across the whole brain (state 1) during the resting-state negatively predicted participants' feelings of social evaluative threat during the stress task; and the mean dwell time of a state characterized by negative correlations between the frontal networks (both left and right) and almost all other networks except the DAN (state 2) predicted participants' subjective stress reports during acute stress. Finally, the fraction of time of state 2 predicted participants' feelings of social evaluation threat and feelings of uncontrollability during acute stress. These dynamic brain states could not, however, predict participants' salivary cortisol response.

State 1 was characterized by positive correlations between the FPN and other networks. Previous studies suggested that the FPN is related to attention allocation, working memory, and cognitive inhibition, which enables participants to flexibly adapt information processing to shifting situational demands [63]. The connections between the FPN, SMN, and VN may reflect the top-down control mechanism that allows the FPN to modulate motion and perception [33]. We found that the longer the dwell time and greater the fraction of time in this CS effectively predicted a reduction in participants' feelings of social evaluative threat, consistent with our hypothesis that top-down regulation could reduce negative emotions. Furthermore, the DMN and FPN were positively correlated. Researchers have found that a positive correlation between the DMN and FPN during rs-fMRI predicts better performances during divergent thinking tasks [64]. This state may reflect participants' ability to regulate attention and emotion toward task demands, rather than toward experimenter monitoring and negative feedbacks. In this way, we infer that brain state 1 could prevent participants from experiencing severe social evaluative threat. Interestingly, state 1 could not predict uncontrollability or subjective stress reports during the stress task, which may be because the feeling of uncontrollability during acute stress was induced by a very difficult task with a short time limit, which was beyond participants' regulation capacity. Moreover, as a component of the stress response, feelings of uncontrollability also induced sufficient subjective stress responses; therefore, state 1 could not predict other stress indicators.

The mean dwell time of state 2 predicted participants' subjective stress reports and the fraction of this state predicted both participants' feelings of uncontrollability and social evaluative threat. Notably, the current results indicated that the mean dwell time of state 2 also marginally predicted social evaluative threat ($\beta = 0.28$, $SE = 0.11$, $p = 0.055$) and feelings of uncontrollability ($\beta = 0.24$, $SE = 0.008$, $p = 0.08$). As mentioned above, state 2 was characterized by negative correlations between the FPN and the whole brain, except the DMN and VAN, whereas the VAN and DMN were positively correlated. This state may promote stress due to dysfunctions between the FPN and other networks. Interestingly, results also showed that in state 2, the DMN was negatively correlated with the DAN, LFN, and RFN, whereas the DAN was positively correlated with the LFN/RFN. In the current study, state 2 was the only state that displayed a strong negative correlation between the DMN and FPN. Previous studies have suggested that the three major brain networks, including the DMN, FPN, and DAN, interact in a top-down manner [65-67]. For example, in the external attention orientation task, the FPN suppressed noise interference from the DMN and positively correlated with activity in the DAN [66,68]. This unique correlation pattern between the DMN, DAN, and FPN represents an external attention orientation state, indicating regulation of goal-directed attention [69,70]. Furthermore, other studies have found that with the increase in task difficulty, the suppression of the FPN on the DMN also increases [71]. These suggest that state 2 is not only an external attention orientation state but also a state that occupies a lot of cognitive resources. In rs-fMRI, participants were asked to look at the cross symbols on the screen, which could be considered as a simple task that does not require the FPN to suppress the DMN. The more that state 2 occurred, the more the effort required by the participant to stay focused. This pattern during rs-fMRI may also reflect the dysfunction of attention, which leads to a stronger stress response.

In addition, states 3 and 4 did not predict the stress response. Similar connectivity patterns are frequently reported in studies using the dynamic functional connectivity approach. State 3 was characterized by hyperconnectivity across almost all brain networks, except for the RFN. Previous large-scale studies have found that children with autism display hyperconnectivity across the entire brain [47,72]. Another study observed hyperconnectivity in patients exhibiting neurological disruption [73]. Other studies using a dynamic approach identified local hyperconnectivity in different mental illnesses [74,75]. Therefore, this state is highly capable of distinguishing patients from healthy populations. State 4 was characterized by weak connections across the whole brain, which have been reported in numerous studies. For example, one study found that weak connectivity among all intrinsic connectivity networks (accounting for 34% of the resting-state scans) was positively correlated with thoughts about oneself during the resting-state scan [44]. A pathological study found that although the weak connectivity overall (accounting for 84% of the resting-state scans) could be found both in major depressive disorder (MDD) and healthy controls, the MDD group had a longer dwell time in such a state [33]. Another pathological study also found that patients with dementia, Lewy bodies, or Alzheimer's disease spent more time than controls in this state of sparse connectivity (accounting for 51% of the resting-state scans) with an absence of strong positive and negative connections [76]. Other studies reported a weak-connection state during the resting state, which always seems to account for the highest proportion of resting-state scans [77]. We consider that this state may reflect the basal reactivity of the resting state.

Our study revealed that dynamic brain activity during the resting state could not predict the participants' endocrine responses to acute stress. This is likely due to the different time scales of different stress responses. For example, subjective emotions are rapidly occurring processes; compared with the emotional response, the endocrine response lags behind temporally. The neural responses associated with these emotional and endocrine responses also demonstrate different temporal dynamics, such as onset time, time to peak, duration, and resurgence after disengagement from the stressor [24]. Many different dynamic approaches can analyze fMRI data on different time scales. It is possible that the dynamic approach we chose here may not fit endocrine data.

Table 4
Validation of the relationship between brain activity and stress response.

Parameter		r	p	95% CI
WL = 60 k = 5	State1_dwell & SET	-0.47***	0.001	[- 0.65, - 0.29]
	State1_frac &SET	-0.43**	0.003	[- 0.63, - 0.22]
	State3_dwell & SSAUCi	0.32*	0.035	[0.08, 0.52]
	State3_dwell & SET	0.2	0.2	[- 0.05, 0.42]
	State3_frac & Uncon	0.27	0.074	[−0.05, 0.49]
WL = 44 k = 4	State4_dwell & SET	-0.56***	0.000	[- 0.70, - 0.40]
	State4_frac &SET	-0.5***	0.001	[−0.69, - 0.26]
	State2_dwell & SSAUCi	0.312*	0.037	[0.01, 0.51]
	State2_frac & SET	0.29	0.056	[−0.02, 0.53]
	State2_frac & Uncon	0.28	0.063	[- 0.10, 0.55]

SSAUCi = the area under the curve with respect to the increase (AUCi) in the seven time-points of subjective stress reports; Uncon = uncontrollability; SET = social evaluation threat, SE = standard error, CI = confident interval , WL = window length.

Future studies may be required to match fMRI data with the endocrine response on various time scales to find the best indicator to predict the endocrine stress response.

Taken together, the results of the current study suggest that brain states in the resting state are characterized as attentional deficits and negative mood, and brain states linking self-control and top-down regulation, may predict the severity of an individual's subjective stress response. To our knowledge, this is the first evidence of individual differences of dynamic brain activity in the resting state predicting the subsequent stress response. However, there were some limitations in the methodology that must also be taken into consideration. First, although dynamic connectivity measures are sensitive to changes in other features of the data, such as variance and signal-to-noise ratio of the fMRI time series and non-stationarity in mean and variance, these confounders may still skew the explanation of the results. Second, the results did not survive Bonferroni correction, which limits the generalizability of these results. Lastly, as the gold standard of the stress response, future studies are needed to explore a reliable way to predict the endocrine stress response, such as a systematic parameter setting for salivary cortisol data, window length, and cluster number.

5. Conclusion

Compared to traditional fMRI analysis methods, the dynamic approach we employed in this study classified resting-state scans into distinct states and calculated the dynamic changes in brain activity between these states. Our results suggested that brain states characterized as attentional deficits and negative mood, and brain states linking self-control and top-down regulation, could predict subjective stress responses in different individuals. These findings provide the first evidence that individual differences in dynamic brain activity in the resting state can predict subsequent stress responses, and provides an objective indicator for detecting an individual's stress response.

CRediT authorship contribution statement

Juan Yang: Writing – review & editing, Conceptualization, Formal analysis. **Yadong Liu:** Writing – original draft, Conceptualization, Formal analysis. **Xi Ren:** Data collecting, Conceptualization, Formal analysis. **Mei Zeng:** Conceptualization, Formal analysis. **Jiwen Li:** Conceptualization, Formal analysis. **Xiaolin Zhao:** Conceptualization, Formal analysis. **Xuehan Zhang:** Conceptualization, Formal analysis.

Acknowledgment

This research was supported by the National Natural Science Foundation of China (31971019), China, Chongqing Research Program of Basic Research and Frontier Technology (cstc2019jcyj-msxmX0016), China, and Fundamental Research Funds for the Central Universities [SWU2009202], China. We are grateful to Xi Ren, Mei Zeng, Jiwen Li, Xiaolin Zhao, Xuehan Zhang for their useful advices and data collection.

Declaration of interest

The authors have no conflicts of interest relevant to this article.

References

[1] R.K. Henderson, H.R. Snyder, T. Gupta, M.T. Banich, When does stress help or harm?The effects of stress controllability and subjective stress response on Stroop performance, Front. Psychol. 3 (2012) 179, https://doi.org/10.3389/fpsyg.2012.00179.

[2] J.A. Penley, J. Tomaka, Associations among the big five, emotional responses, and coping with acute stress, Personal. Individ. Differ. 32 (7) (2002) 1215–1228, https://doi.org/10.1016/S0191-8869(01)00087-3.

[3] K. Vedhara, J. Hyde, I.D. Gilchrist, M. Tytherleigh, S. Plummer, Acute stress, memory, attention and cortisol, Psychoneuroendocrinology 25 (6) (2000) 535–549, https://doi.org/10.1016/S0306-4530(00)00008-1.

[4] S.A. Kiem, K.C. Andrade, V.I. Spoormaker, F. Holsboer, M. Czisch, P.G. Sämann, Resting state functional MRI connectivity predicts hypothalamus-pituitary-axis status in healthy males, Psychoneuroendocrinology 38 (8) (2013) 1338–1348, https://doi.org/10.1016/j.psyneuen.2012.11.021.

[5] R. Shao, W.K.W. Lau, M.K. Leung, T.M.C. Lee, Subgenual anterior cingulate-insula resting-state connectivity as a neural correlate to trait and state stress resilience, Brain Cogn. 124 (2018) 73–81, https://doi.org/10.1016/j.bandc.2018.05.001.

[6] Y. Zhou, Z. Wang, L. Qin, Wan Di, J.Qing Sun, Y. Wen Su, S. Shan Ding, W. Na, J. Rong Xu, Early Altered resting-state functional connectivity predicts the severity of post-traumatic stress disorder symptoms in acutely traumatized subjects, PLoS One 7 (10) (2012), e46833, https://doi.org/10.1371/journal.pone.0046833.

[7] L. de Wandel, M.M. Pulopulos, V. Labanauskas, S. de Witte, M.A. Vanderhasselt, C. Baeken, Individual resting-state frontocingular functional connectivity predicts the intermittent theta burst stimulation response to stress in healthy female volunteers, Hum. Brain Mapp. 41 (18) (2020) 5301–5312, https://doi.org/10.1002/hbm.25193.

[8] M. Yuan, C. Qiu, Y. Meng, Z. Ren, C. Yuan, Y. Li, M. Gao, S. Lui, H. Zhu, Q. Gong, W. Zhang, Pre-treatment resting-state functional mr imaging predicts the long-term clinical outcome after short-term paroxtine treatment in post-traumatic stress disorder, Front. Psychiatry 9 (2018) 532, https://doi.org/10.3389/fpsyt.2018.00532.

[9] D. Dong, M. Duan, Y. Wang, X. Zhang, X. Jia, Y. Li, F. Xin, D. Yao, C. Luo, Reconfiguration of dynamic functional connectivity in sensory and perceptual system in schizophrenia, Cereb. Cortex 29 (8) (2019) 3577–3589, https://doi.org/10.1093/cercor/bhy232.

[10] M. Filippi, E.G. Spinelli, C. Cividini, F. Agosta, Resting state dynamic functional connectivity in neurodegenerative conditions: a review of magnetic resonance imaging findings, Front. Neurosci. 13 (2019) 657, https://doi.org/10.3389/fnins.2019.00657.

[11] C.Y. Wee, S. Yang, P.T. Yap, D. Shen, Sparse temporally dynamic resting-state functional connectivity networks for early MCI identification, Brain Imaging Behav. 10 (2) (2016) 342–356, https://doi.org/10.1007/s11682-015-9408-2.

[12] R. Hindriks, M.H. Adhikari, Y. Murayama, M. Ganzetti, D. Mantini, N.K. Logothetis, G. Deco, Can sliding-window correlations reveal dynamic functional connectivity in resting-state fMRI? NeuroImage 127 (2016) 242–256, https://doi.org/10.1016/j.neuroimage.2015.11.055.

[13] A. Ponce-Alvarez, G. Deco, P. Hagmann, G.L. Romani, D. Mantini, M. Corbetta, Resting-state temporal synchronization networks emerge from connectivity topology and heterogeneity, PLoS Comput. Biol. 11 (2) (2015), e1004100, https://doi.org/10.1371/journal.pcbi.1004100.

[14] A.D. Savva, G.D. Mitsis, G.K. Matsopoulos, Assessment of dynamic functional connectivity in resting-state fMRI using the sliding window technique, Brain Behav. 9 (4) (2019), e01255, https://doi.org/10.1002/brb3.1255.

[15] T.A.W. Bolton, E. Morgenroth, M.G. Preti, D. Van De Ville, Tapping into multi-faceted human behavior and psychopathology using fMRI brain dynamics, Trends Neurosci. 43 (9) (2020) 667–680, https://doi.org/10.1016/j.tins.2020.06.005.

[16] J. Gonzalez-Castillo, P.A. Bandettini, Task-based dynamic functional connectivity: Recent findings and open questions, NeuroImage 180 (2018) 526–533, https://doi.org/10.1016/j.neuroimage.2017.08.006.

[17] R.M. Hutchison, T. Womelsdorf, E.A. Allen, P.A. Bandettini, V.D. Calhoun, M. Corbetta, S. Della Penna, J.H. Duyn, G.H. Glover, J. Gonzalez-Castillo, D. A. Handwerker, S. Keilholz, V. Kiviniemi, D.A. Leopold, F. de Pasquale, O. Sporns, M. Walter, C. Chang, Dynamic functional connectivity: Promise, issues, and interpretations, NeuroImage 80 (2013) 360–378, https://doi.org/10.1016/j.neuroimage.2013.05.079.

[18] A.H.C. Fong, K. Yoo, M.D. Rosenberg, S. Zhang, C.S.R. Li, D. Scheinost, R. T. Constable, M.M. Chun, Dynamic functional connectivity during task performance and rest predicts individual differences in attention across studies, NeuroImage 188 (2019) 14–25, https://doi.org/10.1016/j.neuroimage.2018.11.057.

[19] J. Lim, J. Teng, A. Patanaik, J. Tandi, S.A.A. Massar, Dynamic functional connectivity markers of objective trait mindfulness, NeuroImage 176 (2018) 193–202, https://doi.org/10.1016/j.neuroimage.2018.04.056.

[20] B. yong Park, T. Moon, H. Park, Dynamic functional connectivity analysis reveals improved association between brain networks and eating behaviors compared to static analysis, Behav. Brain Res. 337 (2018) 114–121, https://doi.org/10.1016/j.bbr.2017.10.001.

[21] J. Qin, S.G. Chen, D. Hu, L.L. Zeng, Y.M. Fan, X.P. Chen, H. Shen, Predicting individual brain maturity using dynamic functional connectivity, Front. Hum. Neurosci. 9 (2015) 418, https://doi.org/10.3389/fnhum.2015.00418.

[22] R.P. Viviano, N. Raz, P. Yuan, J.S. Damoiseaux, Associations between dynamic functional connectivity and age, metabolic risk, and cognitive performance, Neurobiol. Aging 59 (2017) 135–143, https://doi.org/10.1016/j.neurobiolaging.2017.08.003.

[23] Y. Tu, A. Tan, Y. Bai, Y.S. Hung, Z. Zhang, Decoding subjective intensity of nociceptive pain from pre-stimulus and post-stimulus brain activities, Front. Comput. Neurosci. 10 (2016) 32.

[24] M.J. Tobia, K. Hayashi, G. Ballard, I.H. Gotlib, C.E. Waugh, Dynamic functional connectivity and individual differences in emotions during social stress, Hum. Brain Mapp. 38 (12) (2017) 6185–6205, https://doi.org/10.1002/hbm.23821.

[25] C.W.E.M. Quaedflieg, V. Van De Ven, T. Meyer, N. Siep, H. Merckelbach, T. Smeets, Temporal dynamics of stress-induced alternations of intrinsic amygdala connectivity and neuroendocrine levels, PLoS One 10 (5) (2015), e0124141, https://doi.org/10.1371/journal.pone.0124141.

[26] K. Dedovic, R. Renwick, N.K. Mahani, V. Engert, S.J. Lupien, J.C. Pruessner, The Montreal Imaging Stress Task: Using functional imaging to investigate the effects of

perceiving and processing psychosocial stress in the human brain, J. Psychiatry Neurosci. 30 (5) (2005) 319–325.
[27] B.M. Kudielka, N.C. Schommer, D.H. Hellhammer, C. Kirschbaum, Acute HPA axis responses, heart rate, and mood changes to psychosocial stress (TSST) in humans at different times of day, Psychoneuroendocrinology 29 (8) (2004) 983–992, https://doi.org/10.1016/j.psyneuen.2003.08.009.
[28] F. Lederbogen, P. Kirsch, L. Haddad, F. Streit, H. Tost, P. Schuch, S. Wüst, J. C. Pruessner, M. Rietschel, M. Deuschle, A. Meyer-Lindenberg, City living and urban upbringing affect neural social stress processing in humans, Nature 474 (7352) (2011) 498–501, https://doi.org/10.1038/nature10190.
[29] A.F.T. Arnsten, K. Rubia, Neurobiological circuits regulating attention, cognitive control, motivation, and emotion: disruptions in neurodevelopmental psychiatric disorders, J. Am. Acad. Child Adolesc. Psychiatry 51 (4) (2012) 356–367.
[30] J. Pan, L. Zhan, C.L. Hu, J. Yang, C. Wang, L. Gu, S. Zhong, Y. Huang, Q. Wu, X. Xie, Q. Chen, H. Zhou, M. Huang, X. Wu, Emotion regulation and complex brain networks: Association between expressive suppression and efficiency in the fronto-parietal network and default-mode network, Front. Hum. Neurosci. 12 (2018) 70, https://doi.org/10.3389/fnhum.2018.00070.
[31] A.-M. Ferrandez, L. Hugueville, S. Lehéricy, J.-B. Poline, C. Marsault, V. Pouthas, Basal ganglia and supplementary motor area subtend duration perception: an fMRI study, Neuroimage 19 (4) (2003) 1532–1544.
[32] B. Giesbrecht, M.G. Woldorff, A.W. Song, G.R. Mangun, Neural mechanisms of top-down control during spatial and feature attention, Neuroimage 19 (3) (2003) 496–512.
[33] Z. Yao, J. Shi, Z.Z.Z. Zhang, W. Zheng, T. Hu, Y. Li, Y. Yu, Z.Z.Z. Zhang, Y. Fu, Y. Zou, W. Zhang, X. Wu, B. Hu, Altered dynamic functional connectivity in weakly-connected state in major depressive disorder, Clin. Neurophysiol. 130 (11) (2019) 2096–2104, https://doi.org/10.1016/j.clinph.2019.08.009.
[34] W.T. McCuddy, L.Y. España, L.D. Nelson, R.M. Birn, A.R. Mayer, T.B. Meier, Association of acute depressive symptoms and functional connectivity of emotional processing regions following sport-related concussion, NeuroImage: Clin. 19 (2018) 434–442, https://doi.org/10.1016/j.nicl.2018.05.011.
[35] W. Zhang, M.M. Hashemi, R. Kaldewaij, S.B.J. Koch, C. Beckmann, F. Klumpers, K. Roelofs, Acute stress alters the 'default' brain processing, NeuroImage 189 (2019) 870–877, https://doi.org/10.1016/j.neuroimage.2019.01.063.
[36] M.J. Domakonda, X. He, S. Lee, M. Cyr, R. Marsh, Increased functional connectivity between ventral attention and default mode networks in adolescents with bulimia nervosa, J. Am. Acad. Child Adolesc. Psychiatry 58 (2) (2019) 232–241.
[37] S.S. Dickerson, M.E. Kemeny, Acute stressors and cortisol responses: a theoretical integration and synthesis of laboratory research, Psychol. Bull. 130 (3) (2004) 355–391, https://doi.org/10.1037/0033-2909.130.3.355.
[38] J. Yuan, Y. Liu, N. Ding, J. Yang, The regulation of induced depression during a frustrating situation: Benefits of expressive suppression in Chinese individuals, PLoS One 9 (5) (2014), e97420.
[39] M. Bukowski, D. Asanowicz, A. Marzecová, J. Lupiáñez, Limits of control: the effects of uncontrollability experiences on the efficiency of attentional control, Acta Psychol. 154 (2015) 43–53, https://doi.org/10.1016/j.actpsy.2014.11.005.
[40] Y. Du, Z. Fu, J. Sui, S. Gao, Y. Xing, D. Lin, M. Salman, M.A. Rahaman, A. Abrol, J. Chen, L.E. Hong, P. Kochunov, E. Osuch, V. Calhoun, NeuroMark: An automated and adaptive ICA based pipeline to identify reproducible fMRI markers of brain disorders, Neuroma.: a Full-.-. Autom. ICA Method identify Eff. fMRI Markers brain Disord. 28 (2019), 19008631, https://doi.org/10.1101/19008631.
[41] M.G. Preti, T.A. Bolton, D. Van De Ville, The dynamic functional connectome: State-of-the-art and perspectives, NeuroImage 160 (2017) 41–54, https://doi.org/10.1016/j.neuroimage.2016.12.061.
[42] A.E. Reineberg, M.T. Banich, Functional connectivity at rest is sensitive to individual differences in executive function: a network analysis, Hum. Brain Mapp. 37 (8) (2016) 2959–2975, https://doi.org/10.1002/hbm.23219.
[43] J. Li, D. Zhang, A. Liang, B. Liang, Z. Wang, Y. Cai, M. Gao, Z. Gao, S. Chang, B. Jiao, R. Huang, M. Liu, High transition frequencies of dynamic functional connectivity states in the creative brain, Sci. Rep. 7 (2017) 46072, https://doi.org/10.1038/srep46072.
[44] H.A. Marusak, V.D. Calhoun, S. Brown, L.M. Crespo, K. Sala-Hamrick, I.H. Gotlib, M.E. Thomason, Dynamic functional connectivity of neurocognitive networks in children, Hum. Brain Mapp. 38 (1) (2017) 97–108, https://doi.org/10.1002/hbm.23346.
[45] A. Patanaik, J. Tandi, J.L. Ong, C. Wang, J. Zhou, M.W.L. Chee, Dynamic functional connectivity and its behavioral correlates beyond vigilance, NeuroImage 177 (2018) 1–10, https://doi.org/10.1016/j.neuroimage.2018.04.049.
[46] D.J.O. Roche, A.C. King, A.J. Cohoon, W.R. Lovallo, Hormonal contraceptive use diminishes salivary cortisol response to psychosocial stress and naltrexone in healthy women, Pharmacol. Biochem. Behav. 109 (2013) 84–90, https://doi.org/10.1016/j.pbb.2013.05.007.
[47] R. Sharma, S.A. Smith, N. Boukina, A. Dordari, A. Mistry, B.C. Taylor, N. Felix, A. Cameron, Z. Fang, A. Smith, N. Ismail, Use of the birth control pill affects stress reactivity and brain structure and function, Horm. Behav. 124 (2020), 104783, https://doi.org/10.1016/j.yhbeh.2020.104783.
[48] C.D. Spielberger, State-trait anxiety inventory, Corsini Encycl. Psychol. (2010) 1.
[49] Beck, A.T., Steer, R.A., Brown, G. (1996). Beck Depression Inventory–II.
[50] J. Wang, X. Wang, M. Xia, X. Liao, A. Evans, Y. He, GRETNA: a graph theoretical network analysis toolbox for imaging connectomics, Front. Hum. Neurosci. 9 (2015) 386, https://doi.org/10.3389/fnhum.2015.00386.
[51] Calhoun, D. Vince, T. Adali, G.D. Pearlson, J.J. Pekar, A method for making group inferences from functional MRI data using independent component analysis, Hum. Brain Mapp. 14 (3) (2001) 140–151.
[52] Rachakonda, S., Egolf, E., Correa, N., Calhoun, V., Neuropsychiatry, O. (2007). Group ICA of fMRI Toolbox (GIFT) Manual. Computer, 554(0959–4388 LA-eng PT-Journal Article PT-Review PT-Review, Tutorial), 304–307. ⟨http://mialab.mrn.org/software/gift/docs/v1.3i_GIFTManual.pdf⟩.
[53] A.J. Bell, T.J. Sejnowski, An information-maximization approach to blind separation and blind deconvolution, Neural Comput. 7 (6) (1995) 1129–1159, https://doi.org/10.1162/neco.1995.7.6.1129.
[54] V.D. Calhoun, T. Adali, G.D. Pearlson, J.J. Pekar, A method for making group inferences from functional mri data using independent component analysis, Hum. Brain Mapp. 16 (2) (2002) 131, https://doi.org/10.1002/hbm.10044.
[55] E.A. Allen, E.B. Erhardt, E. Damaraju, W. Gruner, J.M. Segall, R.F. Silva, M. Havlicek, S. Rachakonda, J. Fries, R. Kalyanam, A.M. Michael, A. Caprihan, J. A. Turner, T. Eichele, S. Adelsheim, A.D. Bryan, J. Bustillo, V.P. Clark, S. W. Feldstein Ewing, F. Filbey, C.C. Ford, K. Hutchison, R.E. Jung, K.A. Kiehl, P. Kodituwakku, Y.M. Komesu, A.R. Mayer, G.D. Pearlson, J.P. Phillips, J.R. Sadek, M. Stevens, U. Teuscher, R.J. Thoma, V.D. Calhoun, A baseline for the multivariate comparison of resting-state networks, Front. Syst. Neurosci. 5 (2011) 2, https://doi.org/10.3389/fnsys.2011.00002.
[56] D. Mantini, M. Corbetta, G.L. Romani, G.A. Orban, W. Vanduffel, Evolutionarily novel functional networks in the human brain? J. Neurosci. 33 (8) (2013) 3259–3275, https://doi.org/10.1523/JNEUROSCI.4392-12.2013.
[57] E.A. Allen, E. Damaraju, S.M. Plis, E.B. Erhardt, T. Eichele, V.D. Calhoun, Tracking whole-brain connectivity dynamics in the resting state, Cereb. Cortex 24 (3) (2014) 663–676, https://doi.org/10.1093/cercor/bhs352.
[58] X. Wu, L. Shi, D. Wei, J. Qiu, Brain connection pattern under interoceptive attention state predict interoceptive intensity and subjective anxiety feeling, Hum. Brain Mapp. 40 (6) (2019) 1760–1773, https://doi.org/10.1002/hbm.24488.
[59] M.A. Ellenbogen, R.J. Carson, R. Pishva, Automatic emotional information processing and the cortisol response to acute psychosocial stress, Cogn. Affect. Behav. Neurosci. 10 (1) (2010) 71–82, https://doi.org/10.3758/CABN.10.1.71.
[60] J.C. Pruessner, C. Kirschbaum, G. Meinlschmid, D.H. %J.P. Hellhammer, Two formulas for computation of the area under the curve represent measures of total hormone concentration versus time-dependent change, Psychoneuroendocrionology 28 (7) (2003) 916–931.
[61] W.R. Shirer, S. Ryali, E. Rykhlevskaia, V. Menon, M.D. Greicius, Decoding subject-driven cognitive states with whole-brain connectivity patterns, Cereb. Cortex 22 (1) (2012) 158–165, https://doi.org/10.1093/cercor/bhr099.
[62] B.B. Gump, P. Stewart, J. Reihman, E. Lonky, T. Darvill, P.J. Parsons, D.A. Granger, Low-level prenatal and postnatal blood lead exposure and adrenocortical responses to acute stress in children, Environ. Health Perspect. 116 (2) (2008) 249–255, https://doi.org/10.1289/ehp.10391.
[63] C.S. Carter, V. Van Veen, Anterior cingulate cortex and conflict detection: an update of theory and data, Cogn. Affect. Behav. Neurosci. 7 (4) (2007) 367–379, https://doi.org/10.3758/CABN.7.4.367.
[64] L. Shi, J. Sun, Y. Xia, Z. Ren, Q. Chen, D. Wei, W. Yang, J. Qiu, Large-scale brain network connectivity underlying creativity in resting-state and task fMRI: cooperation between default network and frontal-parietal network, Biol. Psychol. 135 (2018) 102–111.
[65] M. Corbetta, G. Patel, G.L. Shulman, The reorienting system of the human brain: from environment to theory of mind, Neuron 58 (3) (2008) 306–324, https://doi.org/10.1016/j.neuron.2008.04.017.
[66] M.D. Fox, A.Z. Snyder, J.L. Vincent, M. Corbetta, D.C. Van Essen, M.E. Raichle, The human brain is intrinsically organized into dynamic, anticorrelated functional networks, Proc. Natl. Acad. Sci. U.S.A. 102 (27) (2005) 9673–9678, https://doi.org/10.1073/pnas.0504136102.
[67] R.N. Spreng, The fallacy of a "task-negative" network, 3, 2012, 145.
[68] Buckner, R.L., Andrews-Hanna, J.R., Schacter, D.L. (2008). The Brain's Default Network: Anatomy, Function, and Relevance to Disease.
[69] M. Corbetta, G.L. Shulman, Control of goal-directed and stimulus-driven attention in the brain, Nat. Rev. Neurosci. 3 (3) (2002) 201–215.
[70] L.F. Koziol, Large scale brain systems. The Myth of Executive Functioning, Springer, 2014, p. 15.
[71] M.E. Raichle, A.M. MacLeod, A.Z. Snyder, W.J. Powers, D.A. Gusnard, G. L. Shulman, A default mode of brain function, Proc. Natl. Acad. Sci. U.S.A. 98 (2) (2001) 676–682, https://doi.org/10.1073/pnas.98.2.676.
[72] K. Supekar, L.Q. Uddin, A. Khouzam, J. Phillips, W.D. Gaillard, L.E. Kenworthy, B. E. Yerys, C.J. Vaidya, V. Menon, Brain hyperconnectivity in children with autism and its links to social deficits, Cell Rep. 5 (3) (2013) 738–747, https://doi.org/10.1016/j.celrep.2013.10.001.
[73] F.G. Hillary, C.A. Roman, U. Venkatesan, S.M. Rajtmajer, R. Bajo, N.D. Castellanos, Hyperconnectivity is a fundamental response to neurological disruption, Neuropsychology 29 (1) (2015) 59–75, https://doi.org/10.1037/neu0000110.
[74] A.D. Barber, M.A. Lindquist, P. DeRosse, K.H. Karlsgodt, Dynamic functional connectivity states reflecting psychotic-like experiences, Biol. Psychiatry.: Cogn. Neurosci. Neuroimaging 3 (5) (2018) 443–453, https://doi.org/10.1016/j.bpsc.2017.09.008.
[75] E. Damaraju, E.A. Allen, A. Belger, J.M. Ford, S. McEwen, D.H. Mathalon, B. A. Mueller, G.D. Pearlson, S.G. Potkin, A. Preda, J.A. Turner, J.G. Vaidya, T.G. Van Erp, V.D. Calhoun, Dynamic functional connectivity analysis reveals transient

states of dysconnectivity in schizophrenia, NeuroImage: Clin. 5 (2014) 298–308, https://doi.org/10.1016/j.nicl.2014.07.003.

[76] J. Schumacher, L.R. Peraza, M. Firbank, A.J. Thomas, M. Kaiser, P. Gallagher, J. T. O'Brien, A.M. Blamire, J.P. Taylor, Dynamic functional connectivity changes in dementia with Lewy bodies and Alzheimer's disease, NeuroImage: Clin. 22 (2019), 101812, https://doi.org/10.1016/j.nicl.2019.101812.

[77] F.A. Espinoza, N.E. Anderson, V.M. Vergara, C.L. Harenski, J. Decety, S. Rachakonda, E. Damaraju, M. Koenigs, D.S. Kosson, K. Harenski, V.D. Calhoun, K.A. Kiehl, Resting-state fMRI dynamic functional network connectivity and associations with psychopathy traits, NeuroImage: Clin. 24 (2019), 101970, https://doi.org/10.1016/j.nicl.2019.101970.